ภาคผนวก ก.

บทความทางวิชาการที่นำเสนอใน
การประชุมวิชาการทางวิศวกรรมไฟฟ้า ครั้งที่ 29 (EECON-29)
9-10 พฤศจิกายน 2549 ณ โรงแรมแอมบาสเดอร์จอมเทียน พัทยา จ.ชลบุรี

Frequency Characteristic of Pulse-Echo Signals from Contrast-Assisted Ultrasound

Tosaporn Nilmanee[1], Pornchai Phukpattaranont[2], Nattha Jindapetch[3], Surapon Thienmontri[4]
Department of Electrical Engineering, Faculty of Engineering
Prince of Songkla University, Hatyai, Songkhla, 90112, Thailand
Phone 0-7428-7045 Fax 0-7445-9395, E-mail: tj_spy@hotmail.com[1], pornchai.p@psu.ac.th[2],
nattha.s@psu.ac.th[3], surapon.t@psu.ac.th[4]

Abstract

This article describes frequency characteristic of pulse-echo signals from contrast-assisted ultrasound data. The interaction between the transmitted ultrasound energy and ultrasound contrast agents (UCAs) leads to fundamental and harmonic frequencies scattering, especially the second harmonic. Based on the differences in frequency of ultrasound data from two different media, ultrasound signals are classified into two classes, i.e., UCA and tissue. We show frequency characteristic of UCA signals from an *in vivo* target to demonstrate this nonlinear behavior.

Keywords: ultrasound, contrast agents, harmonic

1. Introduction

Although conventional ultrasound techniques provide excellent clinical and diagnostic information about blood flow in arterial and venous macrovasculature of various systems, the sonographic detection of blood flow in small vessels of the microcirculation is a challenging problem. This is due to the fact that echoes from blood are much smaller than echoes from the surrounding tissue. Moreover, it is limited by other factors such as tissue motion (clutter), attenuation properties of the intervening tissue, and slow or low-volume flow. As a result, the echoes from blood are masked by those from surrounding tissue.

Recently, a significant improvement in blood flow detection by utilizing specific acoustic properties of ultrasound contrast agents (UCAs) has been achieved. That is, methods employing microbubbles provide enhancement in not only blood flow measurement of the backscattered Doppler signals but also gray-scale visualization of the flowing blood in the tissues of organs like the heart, liver, and kidney. Therefore, many reports of the improved diagnostic capabilities exploiting UCAs in clinical applications have been published in the past few years. Examples include improved discrimination between benign and malignant liver tumors [1], improved depiction of the vascularity of cancerous tumors occurring in the liver [2], and enhanced assessment of myocardial perfusion [3].

The objective of this paper is to present frequency characteristic of contrast-assisted ultrasound data from an *in vivo* target. Understanding in frequency responses of pulse-echo signals from UCAs compared with those from surrounding tissue leads to an appropriate design of medical ultrasound imaging modality. The remainder of this paper is organized as follows: Section 2 describes history, development, and acoustic properties of UCAs. The experimental setup, data acquisition, and the method to compute power spectrum are given in Section 3. Results are shown in Section 4. Finally, Conclusions and discussion are provided in Section 5.

2. Background

2.1 History and development of UCAs

An ultrasound contrast agent (UCA) is an external substance that is usually introduced into the vascular system in order to enhance diagnostic and/or therapeutic capabilities in medical ultrasound, e.g. to improve the discrimination between normal and diseased tissue. Interest in UCA research originated from the observation of a cloud of echoes during the intracardiac injection of indocyanine green dye (a substance for measuring blood flow) by Gramiak and colleagues in 1968 while they performed M-mode echocardiography [4]. Afterward, it was discovered that those echoes were caused by microbubbles resulting from cavitation at the catheter tip. Research on finding more appropriate substances to be used as contrast agents in ultrasound has been pursued since that time, but most vigorously in the last 10 years.

Appropriate contrast agents for ultrasound should be small and stable enough to circulate throughout the human body during a typical diagnostic examination. However, contrast agents at the early time fell short on both criteria. Specifically, they could not reach the left heart after an intravenous injection because of the blocking from the capillary circulation in the lungs. This prevented the use of microbubbles as a contrast material in other organs such as the liver and kidney.

In order to extend the lifetime of microbubble contrast agents, many methods have been investigated and several ways to stabilize microbubbles have been discovered. Currently, contrast agents that can survive the blood circulation of the lung are available. The review by Frinking in 2000 reported that three transpulmonary UCAs were approved for clinical use. These are Levovist (Schering AG, Berlin, Germany), Albunex (Molecular Biosystems Inc., San Diago, USA), and Optison (Mallinckrodt, St. Louis, USA) [5]. In addition, more than 10 UCA from various manufacturers are under development and are being investigated for clinical use.

DS09

Most of current ultrasound contrast agents are based on encapsulated microbubbles. Compositions that allow them to traverse the lung capillary bed are the gaseous core with high molecular weights and the stabilized encapsulated shell. Gases with large molecules have low diffusion constants. As a result, their low diffusion rates reduce their dissolvability in fluids, such as blood and water [6]. On the other hand, the encapsulation with lipid or albumin shell prevents inner gases from the swift process of diffusing through the surrounding liquid.

2.2 Acoustic properties of UCAs

The blood pool containing microbubble contrast agent provides significant enhancement in backscattered signals compared with those from normal blood because of their differences in acoustic properties. In addition, When bubbles in a liquid are insonated with ultrasound, they also exhibit oscillatory motion resulting from their stiffness and inertia. While the stiffness of bubbles affects the oscillation of the enclosed gas core like spring, the inertia is caused by the mass of surrounding liquid. This bubble oscillation is important because it makes bubbles act as sound sources resulting in high backscattering enhancement at a specific frequency, referred to as the resonant frequency. The resonance frequency of free gas bubbles can be approximated by [7]:

$$f_r = \frac{1}{2\pi R}\sqrt{\frac{3\gamma \mathrm{P}_0}{\rho}} \qquad (1)$$

where f_r is the resonance frequency, R is the radius of the bubble, P_0 is the pressure, γ is the ratio of specific heat, and ρ is the density of surrounding medium. The formula shows that the resonance frequency is inversely proportional to the bubble radius. Calculations of resonance frequencies of free gas bubbles in water using the following parameters: $\mathrm{P}_0 = 1.01\times10^5$ Pa, $\gamma = 1.4,$ and $\rho = 1000$ kg/m^3, indicate that the bubbles with diameter values from 0.6 μm to 6 μm (typical diameters of contrast microbubbles available currently) provide their resonant frequencies in the frequency range of medical ultrasound (1-10 MHz).

In addition to ultrasound frequency, bubble dynamics varies according to amplitudes of insonating pressure pulse. Characteristics of echoes from interactions between ultrasound and microbubbles can be divided into three categories according to levels of applied acoustic pressures. For the low amplitude pressure excitation, bubbles oscillation is linearly related to applied pressures, thus producing linear backscattered signals. As amplitudes of insonating pressure field increase, bubbles oscillate nonlinearly and produce harmonic echoes, i.e. the fundamental (f_0) and its higher multiple frequencies ($2f_0$, $3f_0$, …) [8-9]. These harmonic frequencies, especially the 2nd harmonic, are significantly higher than those from the surrounding tissue and can be exploited in separating contrast echoes from the surrounding tissue medium.

For insonation at even higher pressures, the coating shells of microbubbles are disrupted and inner gases are dissolved in blood stream leading to suddenly high scattering and highly nonlinear echoes [10]. However, this irreversible process terminates the contrast effect because of bubble destruction. The level of bubble destruction is proportional to the mechanical index (MI), which is defined as [11-12]

$$\mathrm{MI} = \frac{p_-}{\sqrt{f}}, \qquad (2)$$

where MI denotes the mechanical index, p_- is the peak negative pressure measured in MPa, and f is the transmit frequency measured in MHz. The higher the MI used in diagnostic ultrasound system, the higher possibility of bubble destruction. Imaging with low MI values to avoid bubble rupture is important for some imaging targets such as low blood flow organs. If bubbles are destroyed in those targets, low rates of contrast replenishment can interrupt continuous imaging diagnosis. On the other hand, replenishment curves are useful in forming parametric images reflecting function of organs.

3. Materials and Methods

3.1 Experimental setup and data acquisition

The experiment was conducted *in vivo* on a juvenile pig. Bolus injections of SonoVue™, a UCA consisting of sulphur hexafluoride gas bubbles coated by a flexible phospholipidic shell, were administered with concentration 0.01 mL/kg [13]. Three-cycle pulses at 1.56 MHz were transmitted using a convex array probe (CA430E) with mechanical index (MI) 0.158 to scan a kidney of the juvenile pig. RF data were acquired with 16-bit resolution at 20-MHz sampling frequency without TGC compensation and saved for off-line processing. These spend 0.017771 seconds for recording RF data.

3.2 Power Spectrum

After data acquisitions, we determine power spectrum of RF A-lines from the UCA regions as a comparison with those from the tissue regions. Power spectrum of A-line data is obtained using periodogram method with a weighted sequence. The expression used to calculate the power spectrum is given by

$$S\left(e^{j\omega}\right) = \frac{\frac{1}{n}\left|\sum_{i=1}^{n} w_i x_i \; e^{-j\omega i}\right|^2}{\frac{1}{n}\sum_{i=1}^{n}\left|w_i\right|^2} \qquad (3)$$

DS09

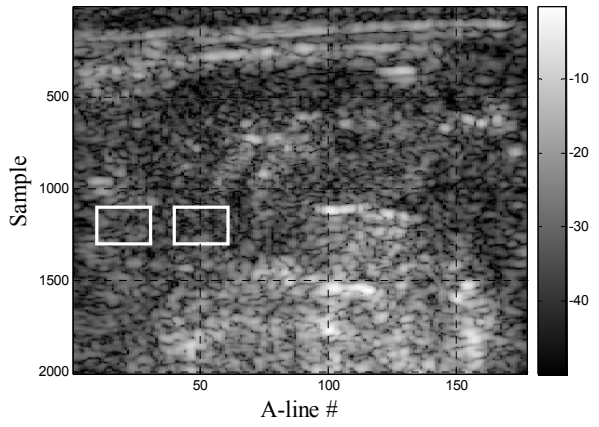

Figure 1 Gray image of a pig's kidney

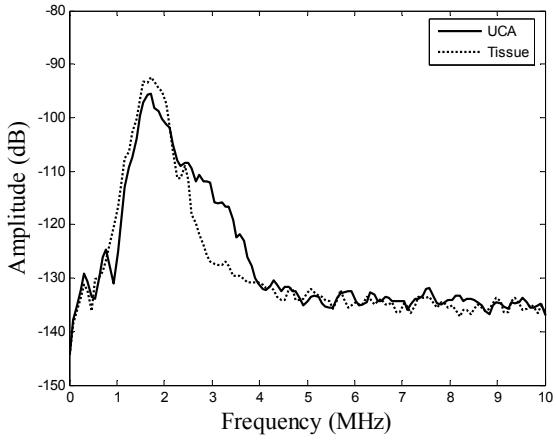

Figure 2 Average spectra of tissue and UCA signals from the left and right boxes of Figure 1

where $S\left(e^{j\omega}\right)$ is the power of a signal, $[x_1, \ldots, x_n]$ is a signal sequence, and $[w_1, \ldots, w_n]$ is a weighted sequence. This expression is an estimate of the power spectrum of signal defined by the sequence $[x_1, \ldots, x_n]$ with the weighted signal sequence by window $[w_1, \ldots, w_n]$. Periodogram uses an n-point FFT to compute the power spectral density (PSD) as $S\left(e^{j\omega}\right)/F$ where F is sampling frequency. The estimated PSD using periodogram algorithm was implemented with MATLAB. We used 21 segments in the region. Each segment contains 201 samples. For this paper, we choose Hanning window as the weighted signal sequence. An n-point symmetric Hanning window is computed by

$$w[k+1] = 0.5\left(1-\cos\left(2\pi\frac{k}{n+1}\right)\right),\ k = 0,\ \ldots,\ n-1 \qquad (4)$$

The PSD estimation represents the distribution of a signal's average power over the range of frequency.

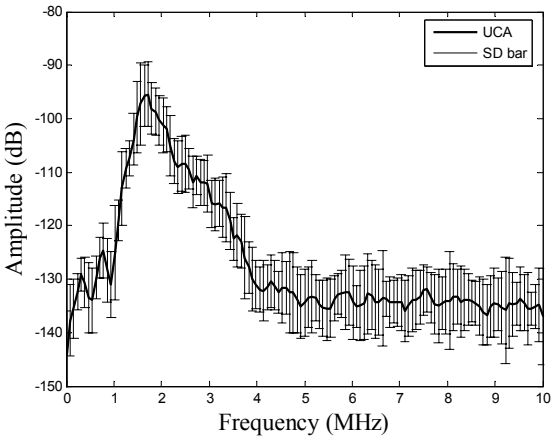

Figure 3 Average spectra and standard deviation (SD) of 21 A-line signals from the UCA region.

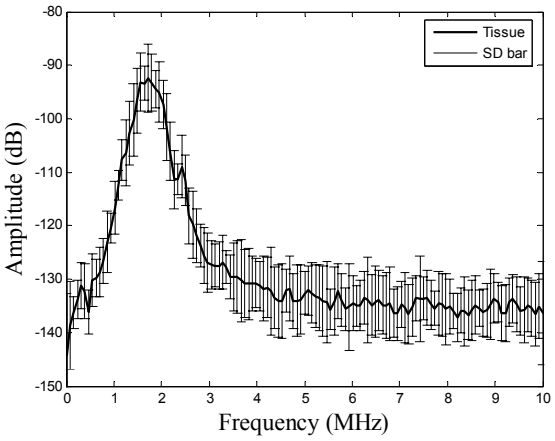

Figure 4 Average spectra and standard deviation (SD) of 21 A-line signals from the tissue region.

To keep estimation simplicity and efficiency, several modifications can be implemented, i.e., averaging over a set of periodograms of (nearly) independent segments, and windowing applied to segments. The multiplication of window in the time domain is convolution in the frequency domain, so some resolution has lost by smearing and spectral leakage. However, the trend of signal's estimated PSD can be enhanced by use of a window function with faster decaying side-lobes.

4. Results and Discussion

The gray image of a pig's kidney is shown in Figure 1 with 50 dB dynamic range. The reference tissue and contrast regions are on the left and right white boxes respectively. Each region consists of pulse-echo signal 21 A-lines.

Average spectra determined from 21 A-line signals of tissue and UCA regions on the left and right boxes of Figure 1 are shown in Figure 2 using dotted and solid lines, respectively. We can see that the harmonic

DS09

spectrum of UCA echoes (solid line) between 2.5 MHz and 4 MHz band are broader than those from tissue echoes (dotted line). This result obviously shows the fundamental and second harmonic frequency generation due to UCAs. On the other hand, the signals from tissue regions contain only the transmitted frequency.

To investigate more details of frequency characteristic of pulse-echo signals, we show average spectra and standard deviation (SD) of 21 A-lines from the UCA and tissue regions in Figure 3 and 4, respectively. We can see that every A-line signal from the UCA region exhibits the second harmonic frequency. On the contrary, the A-line signal from the tissue region contains only the fundamental frequency. These results confirm that the average spectra shown in Figure 2 are a good representation of 21 A-line signals from UCA and tissue regions.

5. Conclusions

We have shown the significant behavior of nonlinearity from interaction between UCA and acoustic energy. The second harmonic frequency of pulse-echo signals from the UCA region is significantly higher than those from the surrounding tissue region. We can utilize average spectra shown in this paper as a reference to design a bandpass filter used for separating UCA signals from tissue signals. The gray image from the second harmonic frequency can improve diagnostic capabilities in clinical applications for both contrast and spatial resolution.

6. Acknowledgement

The authors thank ESAOTE S.p.A, Genova, Italy for supporting the *in vivo* data used in this paper.

References

[1] K. V. Ramnarine, K. Kyriakopoulou, P. Gordon, N. W. McDicken, C. S. McArdle, and E. Leen, "Improved characterization of focal liver tumors: dynamic power Doppler imaging using NC100100 echo-enhancer," *Eur. J. Ultrasound*, vol. 11, no.2, pp. 95-104, May 2000.

[2] S. Tanaka, T. Kitamra, F. Yoshioka, S. Kitamura, K. Yamamoto, Y. Ooura, and T. Imaoka, "Effectiveness of galactose based intravenous contrast medium on color Doppler sonography of deeply located hepatocellular carcinoma," *Ultrasound Med. Biol.*, vol. 21, no. 2, pp. 157-160, 1995.

[3] C. Frischke, J. R. Lindner, K. Wei, N. C. Goodman, D. M. Skyba, and S. Kaul, "Myocardial perfusion imaging in the setting of coronary artery stenosis and acute myocardial infarction using venous injection of a second-generation echocardiographic contrast agent," *Circulation*, vol. 96, pp.959-967, 1997.

[4] R. Gramiak and P. M. Shah, "Echocardiography of the aortic root," *Invest. Radiol.*, vol. 3, pp. 356-366, 1968.

[5] P. J. A. Frinking, A. Bouakaz, J. Kirkhorn, F. J. Ten Cate, and N. de Jong, "Ultrasound contrast imaging: current and new potential methods," *Ultrasound Med. Biol.*, vol. 26, pp. 965-975, 2000.

[6] S. B. Feinstein, P. M. Shah, R. J. Bing, S. Meerbaum, E. Corday, B. L. Chang, G. Santillan, and et al, "Microbubble dynamics visualized in the intact capillary circulation," *J. Am. Coll. Cardiol.*, pp. 595-601, 1984.

[7] N. de Jong, "Improvement in ultrasound contrast agents," *IEEE Eng. Med. Biol. Mag.*, vol. 15, no. 6, pp. 72-82, Nov.-Dec. 1996.

[8] N. De Jong, R. Cornet, and C. T. Lancee, "Higher harmonics of vibrating gas filled microspheres. part one: Simulations," *Ultrasonics*, vol. 32, no. 6, pp. 447-453, 1994.

[9] N. De Jong, R. Cornet, and C. T. Lancee, "Higher harmonics of vibrating gas filled microspheres. part two: Measurements," *Ultrasonics*, vol. 32, pp. 455-459, 1994.

[10] P. J. A. Frinking, N. De Jong, and E. I. Cespedes, "Scattering properties of encapsulated gas bubbles at high ultrasound pressures," *J. Acoust. Soc. Am.*, vol. 105, no. 3, pp. 1989-1996, 1999.

[11] M. A. Averkiou, "Tissue harmonic imaging," *in Proc. IEEE Ultrason. Symp.*, 2000, vol. 2, pp. 1563-1572.

[12] J. E. Chomas, P. Dayton, J. Allen, K. Morgan, and K. W. ferrara, "Mechanisms of contrast agent destruction," *IEEE Trans. Ultrason., Ferroelect., Freq. Contr.*, vol. 48, no. 1, pp. 232-248, Jan. 2001.

[13] M. F. Al-Mistarihi, P. Phukpattaranont and E. S. Ebbini, **"**A Two-Step Procedure for Optimization of Contrast Sensitivity and Specificity of Post-Beamforming Volterra Filgters," *in Proc. IEEE Ultraso. Symp.*, 2004, pp. 978-981.

Tosaporn Nilmanee was born in Thailand in 1981. He received the B. Eng. degree from Prince of Songkla University, Hatyai, Thailand, in 2003. He is currently working toward his M. Eng. degree in Electrical Engineering at Prince of Songkla University. His research interests include ultrasound signal processing, ultrasound contrast imaging.

Pornchai Phukpattaranont Pornchai Phukpattaranont received his B. Eng. and M. Eng. degrees in Electrical Engineering from Prince of Songkla University in 1993 and 1997, respectively. His M. Eng. thesis was on the sequential electrical stimulator for dysphagia patients. In 2004, he obtained his Ph.D. degree in Electrical and Computer Engineering from the University of Minnesota. Since 2004, he has been with the department of Electrical Engineering at Prince of Songkla University. His research interests include ultrasound contrast imaging, signal processing, image processing, and biomedical instrumentation.

ภาคผนวก ข.

บทความทางวิชาการที่นำเสนอใน

PSU-UNS International Conference on Engineering and Environment ICEE-2007

May 10-11, 2007, Phuket Graceland Resort & Spa, Phuket, Thailand

PSU-UNS International Conference on Engineering and Environment - ICEE-2007, Phuket May10-11, 2007
Prince of Songkla University, Faculty of Engineering
Hat Yai, Songkhla, Thailand 90112

DESIGN OF AN OPTIMAL LINEAR BANDPASS FILTER FOR CONTRAST-ASSISTED ULTRASONIC IMAGING

Tosaporn Nilmanee[1], Pornchai Phukpattaranont[2], Nattha Jindapetch[3]
Department of Electrical Engineering, Faculty of Engineering
Prince of Songkla University, Hatyai, Songkhla, 90112, Thailand
Email: tj_spy@hotmail.com[1], pornchai.p@psu.ac.th[2], nattha.s@psu.ac.th[3]

Abstract: *Increasing interest in extending diagnostic capabilities of ultrasound imaging by utilizing ultrasound contrast agents (UCAs) has heightened the need for suitable harmonic separation models. We utilize information from frequency contents of contrast-assisted ultrasound data to improve imaging quality for medical ultrasound purposes. Based on the differences in frequency of ultrasound data from two different media, ultrasound signals are categorized into two classes, i.e. UCA and tissue. In this paper, we use the difference in frequency components of UCA and tissue data as a reference to design a linear bandpass filter (LBF) in order to separating UCA signals from tissue echoes. The LBF is designed using the Parks-McClellan algorithm. We find that appropriate fractional bandwidth (FB) and stopband attenuation of the LBF are 15-25 % and 40-50 dB, respectively. Results show that the images produced from the output signals of optimal LBF are superior to the original B-mode images both in terms of contrast and spatial resolution.*

Key Words: ***Ultrasound Contrast Agents / Harmonic / Linear Bandpass Filter***

1. INTRODUCTION

Modern ultrasonic imaging modalities utilize nonlinear oscillation from ultrasound contrast agents (UCAs) to enhance diagnostic capabilities in medical applications. Radial oscillations of microbubbles due to compressional and rarefactional cycles of the applied pressure are not symmetrical resulting in harmonic echoes, i.e., the fundamental (f_0) and its higher multiple frequencies ($2f_0$, $3f_0$,...) [1]. These harmonic frequencies, especially the 2nd harmonic, are significantly higher than those from the surrounding tissue and can be exploited in the separation of contrast echoes from the surrounding medium. Consequently, many reports of the improved diagnostic capabilities exploiting UCAs in clinical applications have been published. Examples include improved discrimination between benign and malignant liver tumors [2], improved depiction of the vascularity of cancerous tumors occurring in the liver [3], and enhanced assessment of myocardial perfusion [4].

We have recently introduced the frequency characteristics of pulse-echo signals from contrast-assisted ultrasound data. The nonlinear behavior from the interaction between the transmitted ultrasound energy and ultrasound contrast agents (UCAs) leads to fundamental and harmonic frequency scattering, especially the second harmonic. Consequently, ultrasound signals are classified into two classes, i.e., UCA and tissue according to the differences in frequency of ultrasound data from two different media. We have shown in [5] using *in vivo* data that the second harmonic frequency of pulse-echo signals from the UCA region is significantly higher than those from the surrounding tissue region.

In this paper, we employ the difference in frequency component as a reference to design an optimal linear bandpass filter (LBF) in order to separating UCA signals from tissue echoes. The LBF is designed using the the Parks-McClellan algorithm. Fractional bandwidth (*FB*) and stopband attenuation of the LBF are varied and investigated in the design in order to achieve the best filter for enhancing imaging quality both in terms of contrast and spatial resolution.

2. LINEAR BANDPASS FILTER (LBF)

In this paper, we design a linear bandpass filter (LBF) based on the Parks-McClellan algorithm [5]. The designed filters exhibit an equiripple behavior in their frequency response, and hence are also known as equiripple filters. The parameters for the LBP design, i.e. fractional bandwidth and stopband attenuation, are chosen based on the reference spectra of echo signals from UCA and tissue regions. The LBP with optimal parameters should enhance UCA components but suppress tissue signals. While the details of speactral determination are given in [6], parameters to be considered for the LBP are shown in Fig. 1. The fractional bandwidth of the LBF can be obtained by

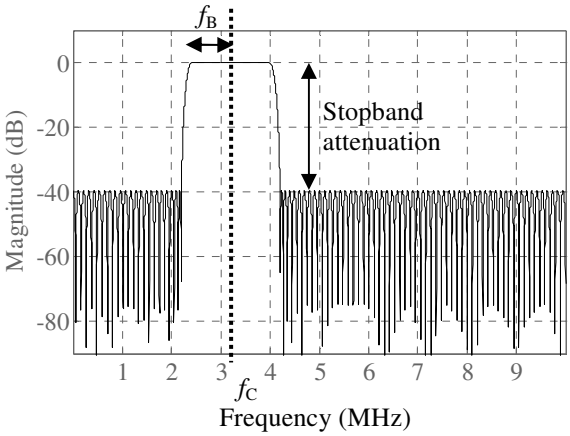

Fig. 1. Two parameters to be considered in the design of an optimal LBP: Fractional bandwidth and stopband attenuation.

$$FB = \frac{2f_B}{f_C} \times 100\% \quad (1)$$

where FB is a fractional bandwidth, f_B is an one-half of defined passband in the filter specification and f_C is a center frequency. In addition, stopband attenuation is defined in term of dB below the passband of filter.

3. MATERIALS AND METHODS

3.1. Experimental setup and data acquisition

The experimental setup and acquisition of ultrasound data used in this paper were described in this section. The experiment was conducted *in vivo* on a juvenile pig. Bolus injections of SonoVue™, a UCA consisting of sulphur hexafluoride gas bubbles coated by a flexible phospholipidic shell, were administered with concentration 0.01 mL/kg [7]. Three-cycle pulses at 1.56 MHz were transmitted using a convex array probe (CA430E) with mechanical index (MI) 0.158 to scan a kidney of the juvenile pig. Ultrasound data were acquired with 16-bit resolution at 20-MHz sampling frequency without TGC compensation and saved for off-line processing.

3.2. Contrast resolution

We measure contrast resolution of images using a contrast-to-tissue ratio (*CTR*), which is given by [8]

$$CTR = 10\log\frac{\overline{P}_C}{\overline{P}_T} \quad (2)$$

where $\overline{P}_C$ and $\overline{P}_T$ are the average power of signals in UCA and tissue regions, respectively. The average power is obtained by

$$\overline{P} = \frac{1}{IJ}\sum_{i=1}^{I}\sum_{j=1}^{J} x_{ij}^2 \quad (3)$$

where x_{ij} is signal in the reference region. We use *CTR* as a measurement of the LBP's capability in extracting second harmonic components.

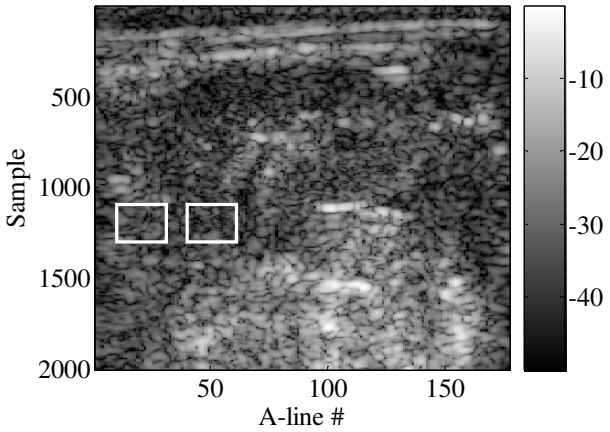

Fig. 2. Gray level image of pig's kidney.

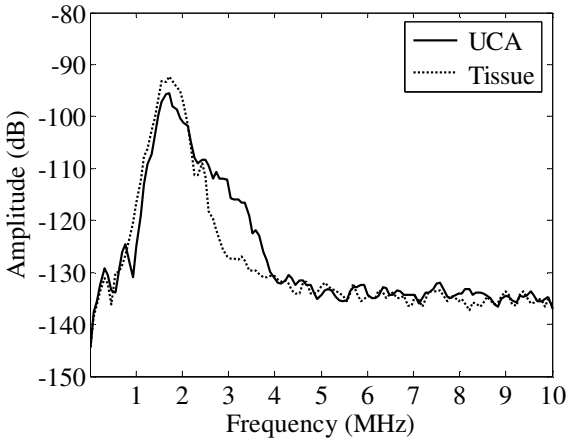

Fig. 3. Average spectra of tissue and UCA signals from the left and right boxes of Fig. 2.

4. RESULTS AND DISCUSSION

The gray image of a pig's kidney is shown in Fig. 2 with 50 dB dynamic range. The reference tissue and UCA regions are on the left and right boxes, respectively. Each region consists of 21 A-line pulse-echo signals. Signal strength from contrast regions inside the kidney is lower than that from tissue regions outside the kidney. This perception is supported by the *CTR* value (-2.1 dB) calculated from equation (2) using the signals in reference boxes. Average spectra determined using 21 A-line signals from tissue and UCA regions in Fig. 1 are shown in Fig. 2 with dotted and solid lines, respectively. We can see that the harmonic spectra of UCA echoes (solid line) between 2.5 MHz and 4 MHz band are broader than those from tissue echoes (dotted line). Based on these average power spectra of UCA over tissue components, we design the optimal LBF to enhance image quality.

We can clearly see in Fig. 3. that the UCA components is higher than the tissue components in the frequency range between 2.5 and 4 MHz. Based on this observation, the center frequency is selected to be 3.2 MHz for all designs of the LBF in this paper. In order to investigate the appropriate stopband attenuation, we design the LBF with fixed fractional bandwidth of 12.5 %. The gray level images of pig's kidney resulting from

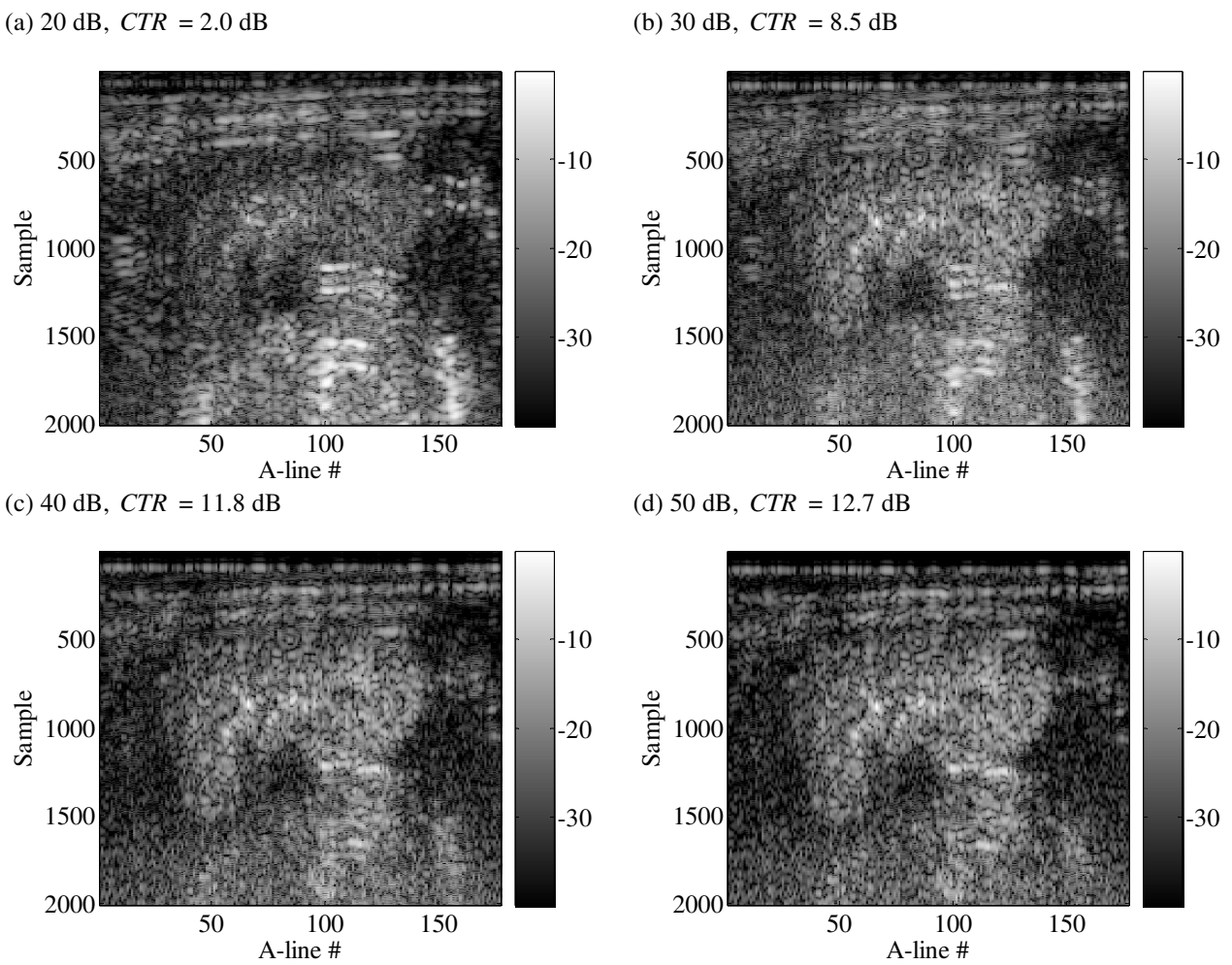

Fig. 4. Gray level images after filtering with the LBF by varying stopband attenuation. *FB* is fixed at 12.5 %.

various stopband attenuations with fixed fractional bandwidth at 12.5 % are shown in Fig. 4. Images, after filtering with the LBF, produced from the stopband attenuation of 20, 30, 40, and 50 dB are shown in Fig. 4(a), (b), (c), and (d), respectively. It is shown that images in Fig.4(c) and (d) have comparable contrast resolution and are better than that from images in Fig. 4(a) and (b). We can clearly visualize the kidney shape and large vascular structures inside the kidney. In addition, *CTR* values from images in Fig. 4(a), (b), (c), and (d) are 2.0, 8.5, 11.8, and 12.7 dB, respectively. These are in agreement with visualized inspection.

Fig. 5 shows gray level images from the LBF with different fractional bandwidth at the fixed stopband attenuation 40 dB. Images, after filtering with the LBF, produced from the *FB* of 10, 10, 25, and 50 % are shown in Fig. 5(a), (b), (c), and (d), respectively. It can be seen that the LBPs with *FB* from 10 % to 25 % are appropriate for enhancing imaging quality in term of contrast resolution. However, spatial resolution is improved when the *FB* of LBF increases. In other words, the LBF with *FB* 25 % provides the best image in term of spatial resolution. In addition, the *CTR* values for the images produced by using appropriate *FB* of the LBF confirm the visualization.

The average spectra from images Fig. 4, which are determined from 21 A-line signals of the same tissue and UCA regions as in Fig. 1, are shown in Fig. 6. Due to the increase in stopband attenuation of the LBF, the second harmonic components in Fig.6(c) and (d) are significantly higher than those from the fundamental frequency. As a result, the imaging quality in term of contrast resolution is improved. Similarly, we have shown the power spectral density of tissue and UCA regions of the images from Fig. 5 in Fig.7. It is noticable that the second harmonic components in Fig. 7(a), (b) and (c) are high compared to the fundamental frequency.

5. CONCLUSIONS

We utilize the second harmonic components due to UCA for enhancing imaging quality of medical ultrrasound images. Gray level images produced using the LBF with optimal fractional bandwidth and stopband attenuation is better than original B-mode images both in terms of contrast and spatial resolution. In the design of the LBF, the appropriate stopband attenuation and *FB* are found to be 40-50 dB and 15-25 %, respectively.

6. ACKNOWLEDGMENS

The authors thank ESAOTE S.p.A, Genoa, Italy for supporting the *in vivo* data used in this paper.

(a) *FB* = 10 %, *CTR* = 11.2 dB

(b) *FB* = 15 %, *CTR* = 11.4 dB

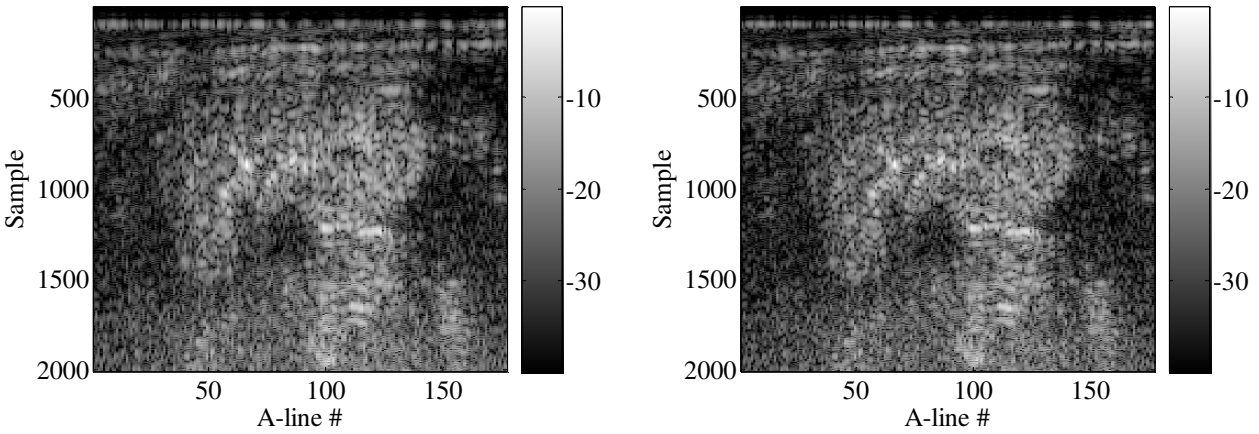

(c) *FB* = 25 %, *CTR* = 11.0 dB

(d) *FB* = 50 %, *CTR* = 2.8 dB

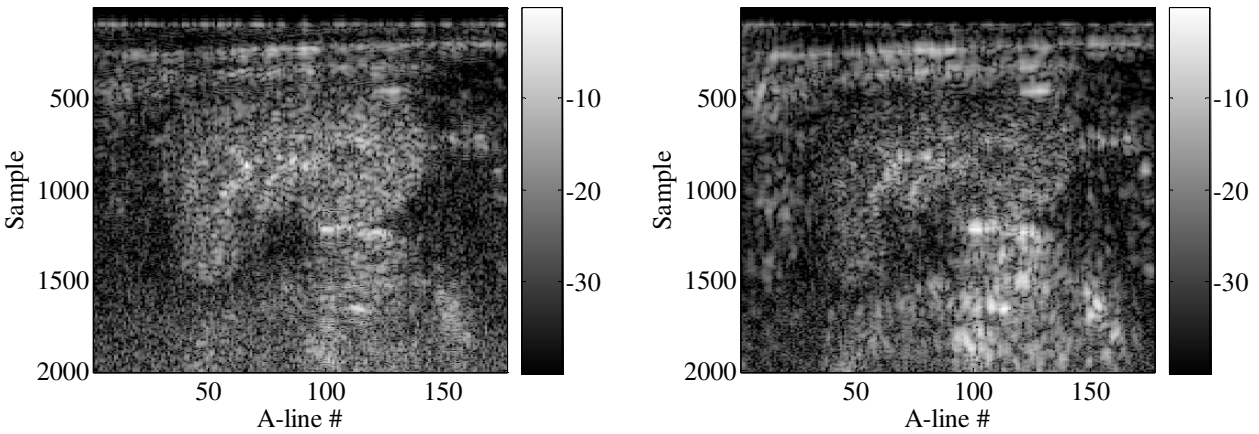

Fig. 5. Gray level images of pig's kidney after filtering with various *FB*. Stopband attenuation is fixed at 40 dB.

7. REFERENCES

[1] N. De Jong and R. Cornet and C. T. Lancee, "Higher harmonics of vibrating gas filled microspheres. Part two: Measurements," *Ultrasonics*, vol. 32, no. 6, pp.455-459, 1994.

[2] K. V. Ramnarine, K. Kyriakopoulou, P. Gordon, N. W. McDicken, C. S. McArdle, and E. Leen, "Improved characterization of focal liver tumors: dynamic power Doppler imaging using NC100100 echo-enhancer," *Eur.J. Ultrasound*, vol. 11, no.2, pp. 95-104, May 2000.

[3] S. Tanaka, T. Kitamra, F. Yoshioka, S. Kitamura, K. Yamamoto, Y. Ooura, and T. Imaoka, "Effectiveness of galactose based intravenous contrast medium on color Doppler sonography of deeply located hepatocellular carcinoma," *Ultrasound Med. Biol.*, vol. 21, no. 2, pp. 157-160, 1995.

[4] C. Frischke, J. R. Lindner, K. Wei, N. C. Goodman, D. M. Skyba, and S. Kaul, "Myocardial perfusion imaging in the setting of coronary artery stenosis and acute myocardial infarction using venous injection of a second-generation echocardiographic contrast agent,"*Circulation*, vol. 96, pp.959-967, 1997.

[5] S. K. Mitra, *Digital Signal Processing: A Computer-Based Approach*, McGraw-Hill, New York, 2 edition, 2001.

[6] T. Nilmanee, P. Phukpattaranont, N. Jindapetch and S. Thienmontri, "Frequency Characteristic of Pulse-Echo Signals from Contrast-Assisted Ultrasound," *29th Electrical Engineering Conference (EECON-29)*, November, 2006, Vol.2, pp. 949-952.

[7] M. F. Al-Mistarihi, P. Phukpattaranont and E. S. Ebbini, "A Two-Step Procedure for Optimization of Contrast Sensitivity and Specificity of Post-Beamforming Volterra Filgters," *in Proc. IEEE Ultraso. Symp.*, 2004, pp. 978-981.

[8] M. F. Al-Mistarihi, P. Phukpattaranont and E. S. Ebbini, "Post-Beamforming Third-order Volterra Filter (ThOVF) for Pulse-echo Ultrasonic Imaging," *ICASSP*, 2004, vol. 3, pp. 97-100.

(a) 20 dB

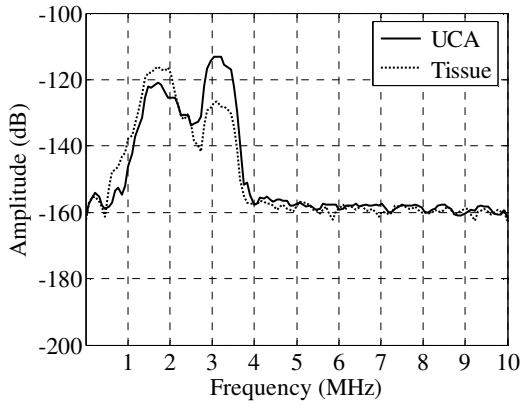

(b) 30 dB

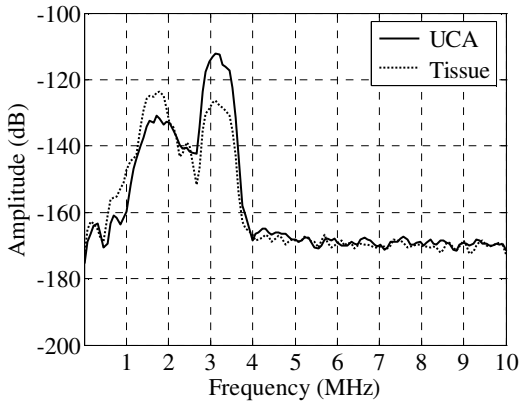

(c) 40 dB

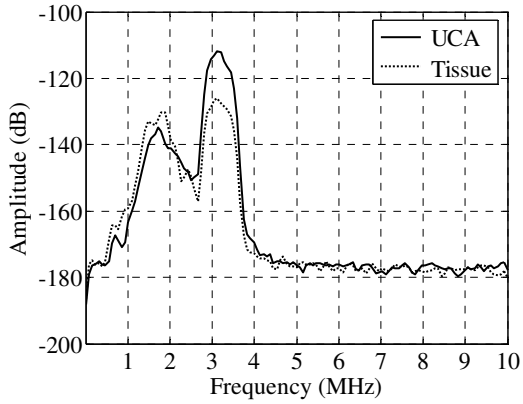

(d) 50 dB

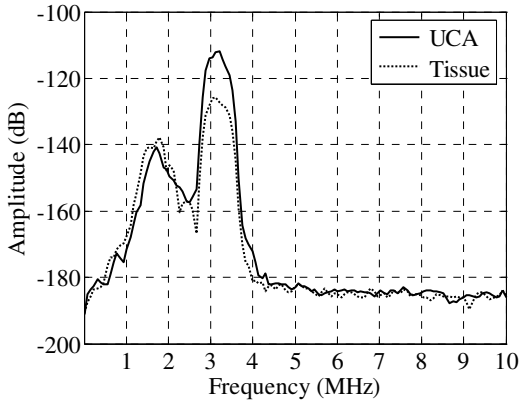

Fig. 6. Power spectra density of gray level images after filtering with LBF by varying stopband attenuation.

(a) *FB* = 10 %

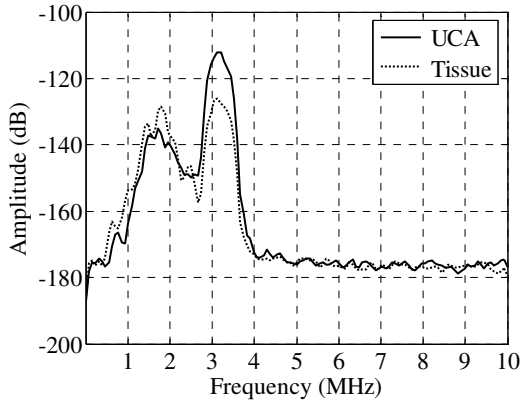

(b) *FB* = 15 %

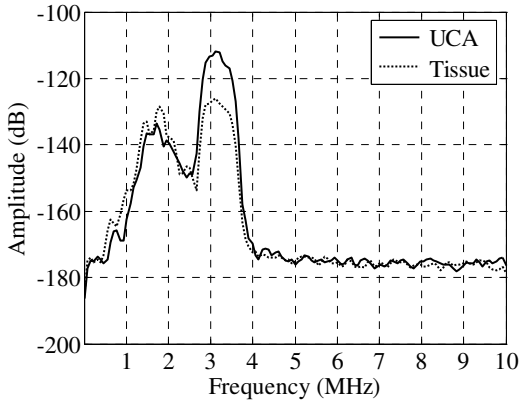

(c) *FB* = 25 %

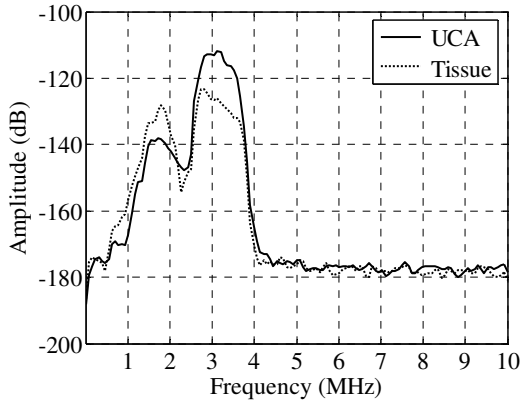

(d) *FB* = 50 %

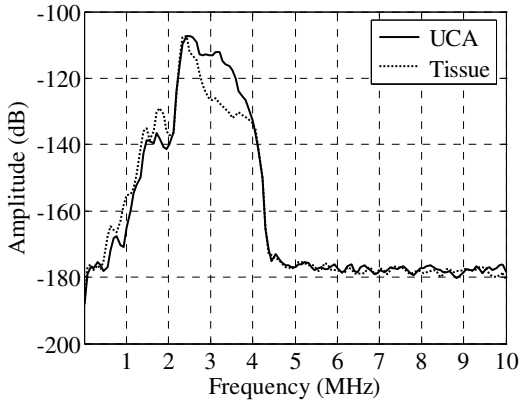

Fig. 7. Power spectra density of the gray level images after filtering with LBF with various *FB*.